Switching behavior of a Stoner particle beyond the relaxation time limit

M. Bauer, J. Fassbender, and B. Hillebrands
Fachbereich Physik und Forschungsschwerpunkt Materialwissenschaften Erwin-Schrödinger-Straße 56 Universität Kaiserslautern, 67663 Kaiserslautern, Germany

R. L. Stamps
Department of Physics, University of Western Australia, Perth, Australia

We report results of the switching properties of Stoner-like magnetic particles subject to short magnetic field pulses, obtained by numerical investigations. We discuss the switching properties as a function of the external field pulse strength and direction, the pulse length and the pulse shape. For field pulses long compared to the ferromagnetic resonance precession time the switching behavior is governed by the magnetic damping term, whereas in the limit of short field pulses the switching properties are dominated by the details of the precession of the magnetic moment. In the latter case, by choosing the right field pulse parameters, the magnetic damping term is of minor importance and ultrafast switching can be achieved. Switching can be obtained in an enlarged angular range of the direction of the applied field compared to the case of long pulses.

Introduction

Switching the direction of magnetization of magnetic particles by an external magnetic field is one of the fundamental issues in magnetic data storage. The switching process described by the Gilbert form of the Landau-Lifschitz equation has been studied only in special cases for a narrow range of magnetic field geometries [1-3]. For a static applied field, switching by homogeneous rotation of the magnetization and by nucleation and propagation of domain walls, and by combinations thereof, have been studied thoroughly [1,4]. Nowadays magnetic device applications demand a deeper insight into the switching dynamics introduced by magnetic field pulses, especially on the time scale where the length of the field pulse is comparable or shorter than the typical relaxation time of the magnetization. Here dynamic effects dominate the switching behavior, and, in addition to parameters like the strength and direction of the applied field pulse, its length and shape are important.

The subject of this paper is to present (i) an overview of the fundamental switching mechanisms possible for different sample geometries in static and pulsed magnetic fields, and (ii) to study in detail the magnetic switching behavior of thin ellipsoidal Stoner-like particles by numerical simulation, subject to short external field pulses. We perform the studies in the Stoner limit, i.e., we assume a homogeneous magnetization, constant in strength and direction across the particle. Results of inhomogeneous magnetization distributions will be the subject of a forthcoming publication [5]. Our results apply to the switching properties of small magnetic grains in a data storage medium, as well as to sensors and magnetic random access memory (MRAM) cells in the limit of small geometries.

Model

The magnetic sample of homogeneous magnetization is characterized by the demagnetizing factors in x-, y- and z-direction N_x, N_y, and N_z. Since we only consider spherically or ellipsoidally shaped finite samples or infinite films the demagnetizing field is constant across the sample. For simplicity and an easy comparison between the results all calculations are performed for permalloy (saturation magnetization $4\pi M_S = 10.8$ kG, gyromagnetic factor $\gamma = 0.0176/(\text{Oe·ns})$, Gilbert magnetic damping factor $\alpha = 0.008$ [6,7]). Shape and uniaxial in-plane anisotropy are assumed. Except for the sphere the demagnetizing factors or the anisotropy constant are chosen such that the magnetization will lie in the xy-plane (in-plane). For all in-plane anisotropies the x-axis corresponds to the easy axis of magnetization. In all cases the initial magnetization direction is along the −x-direction.

The motion of the magnetic moment under the influence of an effective magnetic field including a phenomenological damping mechanism is described by the Landau-Lifschitz equation (LL) [8]

$$\frac{\partial \vec{M}}{\partial t} = -\gamma \vec{M} \times \vec{H}_{\text{eff}} - \frac{\gamma\alpha}{M_S} \vec{M} \times \left(\vec{M} \times \vec{H}_{\text{eff}}\right). \quad (1)$$

Eq. (1) was modified by Gilbert (LLG) [9] to

$$\frac{\partial \vec{M}}{\partial t} = -\gamma \vec{M} \times \vec{H}_{\text{eff}} + \frac{\alpha}{M_S} \vec{M} \times \frac{\partial \vec{M}}{\partial t} \quad (2)$$

to overcome the unphysical solution of the LL equation for large damping parameters α [10]. Hence, in our calculations the LLG equation is used. The first term on the right hand side of Eq. (2) is the precession term and the second the damping term. The effective field $\vec{H}_{\text{eff}}$ is defined by the sum of all fields acting on the magnetization

$$\vec{H}_{\text{eff}} = \vec{H}_{\text{ext}} + \vec{H}_{\text{ani}} + \vec{H}_{\text{shape}}$$

$$\vec{H}_{\text{ani}} = \left|\vec{H}_{\text{ani}}\right| \frac{M_x}{M_s} \hat{x} \quad (3)$$

$$\vec{H}_{\text{shape}} = -\left(4\pi N_x M_x \hat{x} + 4\pi N_y M_y \hat{y} + 4\pi N_z M_z \hat{z}\right)$$

with $\vec{H}_{\text{ext}}$ the external applied field, $\vec{H}_{\text{ani}}$ the uniaxial anisotropy field with x the easy axis of magnetization, N_i ($i = x,y,z$) the diagonal components of the demagnetization tensor in diagonal form, and M_x, M_y and M_z the vectorial magnetization components along the x-, y- and z-axes. The results are obtained by straight forward numerical integration of Eq. (2) using an embedded Runge-Kutta algorithm [11].

Precession of the magnetization in a static applied field

To illustrate the influence of the magnetic damping parameter, as well as the shape and uniaxial anisotropy on the switching behavior let us discuss first the simple case of an

isotropic sphere and second of an infinite film, when a static magnetic field is applied.

Figs. 1 and 2 show the salient features in the three-dimensional time evolution of the direction of magnetization for various scenarios. We assume that initially the direction of magnetization is along the –x-direction, and that a static field of $\vec{H}_{ext} = 50$ Oe (gray arrow) is instantly applied at the time $t_0 = 0$ in the xy-plane with an angle of 135° with respect to the initial direction of $\vec{M}$ (black arrow). In the case of an isotropic sphere the demagnetizing factors are $N_x = N_y = N_z = 1/3$. Without damping, i.e., in absence of a mechanism of energy dissipation, and without anisotropy the Zeeman energy of the magnetization remains constant and the magnetization will start to precess in a circular orbit with its plane perpendicular to $\vec{H}_{ext}$, as displayed in Fig. 1(a). No switching will appear. If the external field is instantly switched off at the time $t_1 > t_0$, the magnetization will rest at the direction $\vec{M}(t_1)$, since for $t > t_1$ the magnetization direction is parallel to the effective field $\vec{H}_{eff}$. If a uniaxial anisotropy ($H_{ani} = 45\,Oe$) is present (Fig. 1 (b)) the circular orbit of the magnetization is deformed in order to keep the magnetization closer to the x-axis but still no switching occurs. Note that now the path of the magnetization vector does not lie in a plane. If the external field again is instantly switched off at t_1 the magnetization will precess about the axis of the anisotropy field for $t > t_1$ starting at the position $\vec{M}(t_1)$. Next a small damping parameter of $\alpha = 0.008$ is assumed. Figure 1(c) shows the time evolution of the magnetization for a sphere without anisotropy for the first 500 ns. The switching of the magnetization occurs only due to the damping term in the LLG equation. Since the value of the damping parameter

is very small 500 ns are not sufficient to align the magnetization parallel to the applied field. If now again a uniaxial anisotropy is considered (Fig. 1 (d)) the switching process proceeds faster. After 500 ns the switching process is nearly completed. To summarize Fig. 1: Switching occurs for static applied fields only due to the damping term of the LLG equation and anisotropy accelerates the switching speed. The role of anisotropy in this acceleration cannot be replaced by increasing the applied field value.

Next we consider an infinite, thin film with $N_x = N_y = 0$, $N_z = 1$, i.e., the xy-plane is the film plane. The results are displayed in Fig. 2. As above, the magnetization is initially aligned along the –x-direction prior to the application of the external field of 50 Oe. Since the external field is applied in the film plane, the precession orbit is mostly outside the film plane, and hence a demagnetizing field will appear. This field is strong due to the z-demagnetizing factor $N_z = 1$. The precession orbit is now strongly deformed and the magnetization is almost forced into the film plane, as displayed in Fig 2 (a). The orbit consists of two arc-like sections almost parallel to the film plane. By choosing an appropriate termination time, t_1, for the static magnetic field, a large range of final in-plane angles of the magnetization can be realized. If a uniaxial anisotropy field of 45 Oe is considered (Fig. 2 (b)) the precession behavior of the magnetization remains nearly the same, only the range of accessible in-plane magnetization angles is reduced. However, the magnetization crosses the hard in-plane axis, and, for an appropriate termination time of the applied field, the switching of the magnetization to the +x direction may occur due to the precession term of the LLG equation. Even with a reduced applied field of 18 Oe a crossing of the hard in-plane axis is possible (not shown in Fig. 2). If we now consider again a small damping parameter of $\alpha = 0.008$ for a film without (Fig. 2 (c)) and with (Fig. 2 (d)) anisotropy, the magnetization switches to the direction of the applied or effective field, respectively,
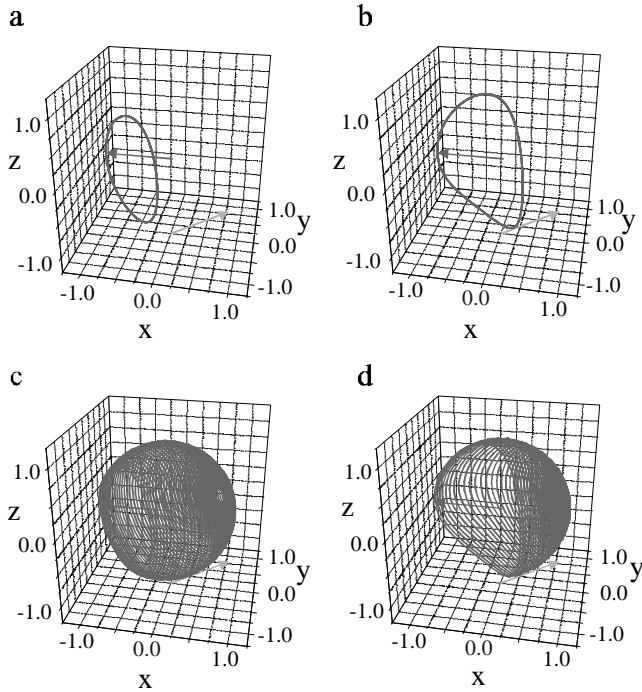

Figure 1: Three-dimensional time evolution of the direction of magnetization of a permalloy sphere. The initial direction of magnetization is along the –x-direction (black arrow); a field of 50 Oe (gray arrow) is applied at an angle of 135° in the xy-plane. The time evolution is shown for the first 500 ns. a) no anisotropy, no damping, b) uniaxial anisotropy field 45 Oe, no damping, c) no anisotropy, damping parameter $\alpha = 0.008$, d) uniaxial anisotropy field 45 Oe, damping parameter $\alpha = 0.008$.
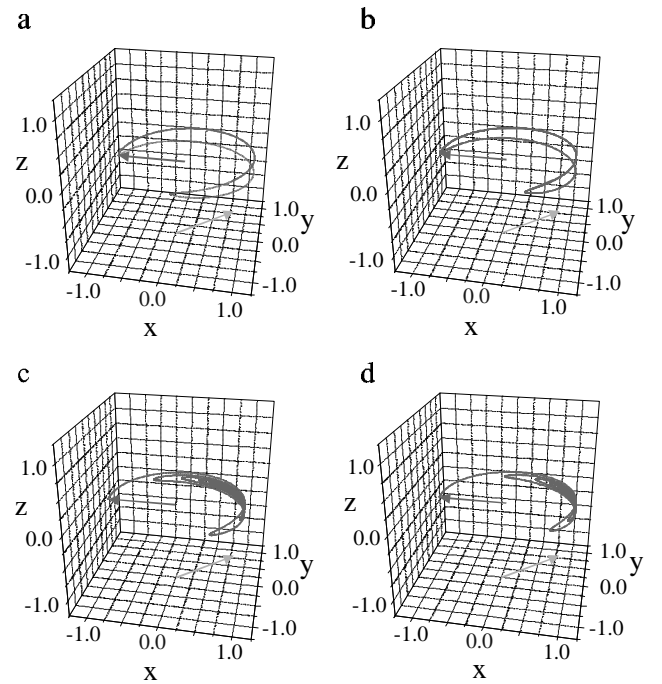

Figure 2: Three-dimensional time evolution of the direction of magnetization of a thin infinitely extended magnetic permalloy film. The time evolution is shown for the first 10 ns. All other parameters as in Fig. 1.

within the first 5 ns, as shown in both graphs. The conclusion of this paragraph is that due to the large demagnetizing field the switching of the magnetization in a film with damping occurs very fast compared to a sphere and that switching without damping should be possible in principle if a pulsed magnetic field is applied instead of a static one.

Precession of the magnetization in a pulsed applied field
We will now discuss the more complex switching phenomena upon application of a magnetic field pulse. To define the notation of the pulse rise time, pulse length and pulse fall time used throughout this article a scheme of the field pulse is shown in Fig. 3. The pulse is characterized by the triplets of numbers "rise time / pulse length / fall time". For the pulse rise and fall a sinusoidal time dependence is assumed. All values are given in units of nanoseconds.

In Fig. 4 different scenarios of the magnetization switching including damping initiated by a 0.2/1.0/0.2 magnetic field pulse are shown for a film without (a) and with (b) anisotropy. All parameters but the shape of the pulse are the same as in Fig. 2 (c) and (d). Figures 4 (c) and (d) show the corresponding results for an ellipsoidally shaped particle with the demagnetization factors of $N_x = 0.008$, $N_y = 0.012$ and $N_z = 0.980$. As in section III the initial direction of magnetization (black arrow) is along the −x-direction; a field of 50 Oe (gray arrow) is applied at an angle of 135° in the xy-plane. The time evolution is shown for the first 10 ns. Let us first discuss the simple case of a film without anisotropies (a). The magnetic field pulse leads to a damped precession about the effective field direction. At the time, at which the applied field terminates (during the field pulse the data are represented black, afterwards gray), the z-component of the magnetization is likely nonzero and hence the field due to the shape anisotropy (perpendicular to the film plane) acts on the magnetization leading to the relaxation of the magnetization into the film plane on a circular orbit around the z-axis. Since no in-plane anisotropy is present remarkably all in-plane angles of the magnetization can be realized as a final state.

Next we discuss the influence of a uniaxial in-plane anisotropy (b). The time evolution of the magnetization during the time the field pulse is applied is similar to (a). Only the effective field is modified by the anisotropy field and hence the axis of precession is altered. Therefore, in contrast to (a), not only the demagnetizing field but also the anisotropy field is present leading to a break in symmetry with respect

to the yz-plane. Roughly the magnetization relaxes to the easy in-plane direction which is closer to the magnetization at the time the field pulse terminates. To be precise energy consideration has to be taken into account leading to an instability region close to the y-axis, discussed below.
In Fig. 4 (c) the demagnetizing factor is chosen such that the uniaxial in-plane component is comparable to that of Fig. 4 (b) (see above). Nevertheless the switching behavior is different. After switching the magnetization during the field pulse, the magnetization returns to its initial position after termination of the field pulse. The origin of this behavior can be understood on the basis of the modification of the z-component of the demagnetizing field. For an ellipsoid this component is smaller compared to a thin film. Hence the magnetization is not so strongly forced into the in-plane direction. Consequently the time in which the track of the magnetization is located in the x < 0 halfspace is increased leading to an increased probability of switching back to the initial direction depending on the pulse termination time compared to the film. By choosing adequate values of the demagnetizing factors a continuous transition between the switching behavior of a sphere and a film can be obtained.
Figure 4 (d) shows the time evolution of the magnetization reversal for a ellipsoidally shaped sample with uniaxial anisotropy. Although the sum of both uniaxial in-plane anisotropy contributions is ≈ 90 Oe, fast and stable switching occurs for a field pulse of 50 Oe.
After the discussion of the different contributions to the switching behavior of the magnetization, especially for short magnetic field pulses, we will now study in more detail the role of the field pulse length and shape for the ellipsoidally

Figure 4: Different scenarios of the magnetization switching initiated by a 0.2/1.0/0.2 magnetic field pulse shown for a thin film without (a) and with (b) anisotropy ($H_{ani} = 45$ Oe). (c) and (d) show the corresponding results for an ellipsoidally shaped particle with the demagnetization factors of $N_x = 0.008$, $N_y = 0.012$ and $N_z = 0.980$. The initial direction of magnetization is along the −x-direction (black arrow); a field of 50 Oe (gray arrow) is applied at an angle of 135° in the xy-plane. The time evolution is shown for the first 10 ns. Data are represented black (gray) during (after) the magnetic field pulse
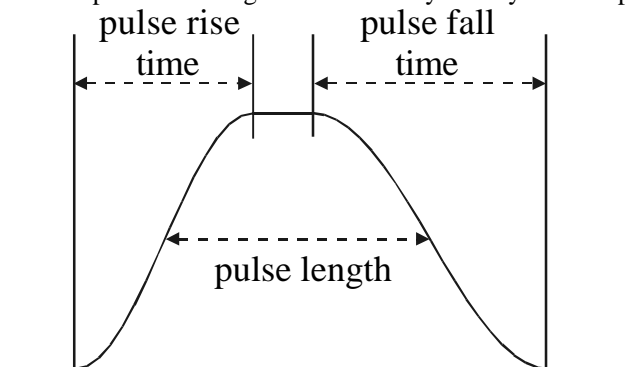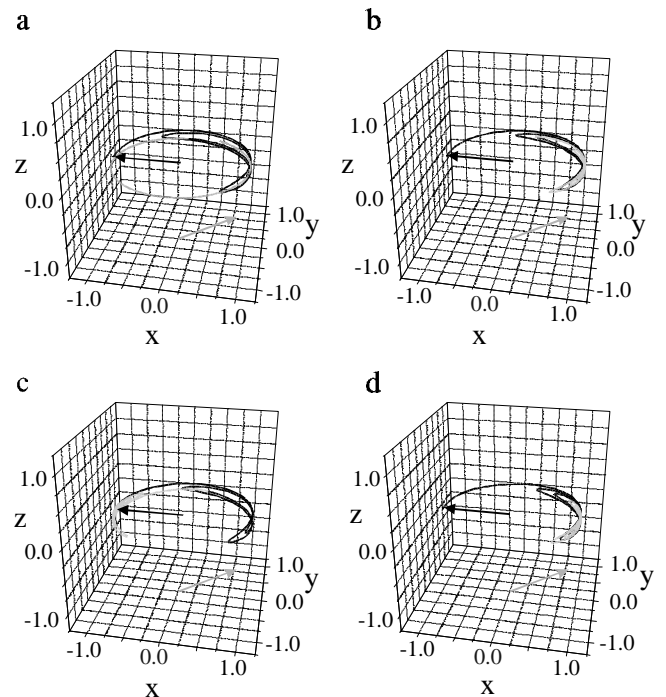

Figure 3: Scheme of the magnetic field pulse to explain the parameters pulse rise time/pulse length/pulse fall time. All values are given in units of nanoseconds. Rise and fall times have a sinusoidal shape, the pulse length is determined as the full width at half maximum.

shaped sample without additional anisotropies, first discussed in Fig. 4 (c).

From Figs. 4 (b) and (c) it becomes immediately clear, that the length of a short pulse determines the final state of the magnetization. It should be noted that experimental evidence for this was recently demonstrated by Back *et al.*, testing the domain structure written into a perpendicularly magnetized film by a pulse of high energy electrons propagating at near speed of light in the Stanford Linear Accelerator Facility [12]. In their experiments it was possible to observe the different domain patterns created by different magnetic field pulse lengths.

Magnetization switching of small particles

Since, in the following, we are mostly interested in the final state of the magnetization, we will use a special graphical representation, providing the final state information as a function of the pulse field strength and direction. Figure 5 shows such a diagram for a 0.0/2.75/0.0 field pulse (rectangular shape). As a result of the ellipsoidal shape with the demagnetizing factors $N_x = 0.008$, $N_y = 0.012$ and $N_z = 0.980$ the magnetization is aligned either in the $+x$- or the $-x$-direction at zero field. Prior to the field pulse the magnetization is aligned in the $-x$-direction. Dark areas in Fig. 5 indicate, that the final state of magnetization is in the $-x$-direction. Bright areas indicate a successful switching into the $+x$-direction. The circular coordinate system indicates the direction and strength of the field pulse. The strength is zero at the center, and its increment is 25 Oe between two circles. The direction from the center indicates the direction of the external field.

Switching with long pulses − the relaxation dominated switching regime

We now apply a 0.0/2.75/0.0 pulse. The result is displayed in Fig. 5. First, it is evident, that switching takes place for most of the parameter sets, where the field direction has a component along the $+x$-direction. If the field is aligned near the $\pm y$-directions, switching and non-switching areas alternate with increasing field strength (instability region). This can be easily understood by the fact, that during the precession about the field in y-directions the x-component of the magnetization oscillates in time between the $+x$- and the $-x$-direction. The final state is determined by the position of the magnetization at the time, at which the field pulse is terminated, $\bar{M}(t_1)$. For almost all cases, it is sufficient to consider only the x-component of the magnetization. Since the field strength increases with distance from the center, the precession frequency will do so as well, and the actual position of the magnetization at the time of pulse termination depends sensitively on that time resulting in alternating orientations of the magnetization in the final state. This instability region is due to a beating between the applied field pulse and the precession of the magnetization. Again, in almost all cases it is sufficient to consider only the x-component of the magnetization to determine its final state.

The four diagrams labeled (a) to (d) in Fig. 5 show the time evolution of the three mutual magnetization components at different values of field strength and direction. We observe a significant ringing of the magnetization upon both at beginning and termination of the external field pulse. In all

cases the crucial parameter for the switching is the magnetic damping parameter. If the applied field pulse has a component along the $+x$-direction (Fig. 5, points b and c) the damping promotes the switching because the average of the x-component (bold black line) in a single oscillation period moves toward the $+x$-direction. Otherwise the damping hinders the switching because the $-x$-direction is favored.

It is evident from Fig. 5, that for a too small value of the applied field no switching will appear. The diagram might serve to identify the parameters for optimum switching in, e.g., a MRAM storage cell geometry, usually consisting of a magnetic multilayer stack containing the storage element we are discussing here and the sensor structure for read-out, and of two crossing, current-carrying wires to address and switch the cell. For the moment we assume that both wires are perpendicular to each other, and they are aligned parallel and perpendicular to the easy axis of the storage elements. Each wire alone is supposed not to switch any storage elements. Only the addressed element beneath two current carrying wires will be switched. From Fig. 5 crucial information is extracted about the switching by drawing a square (for same
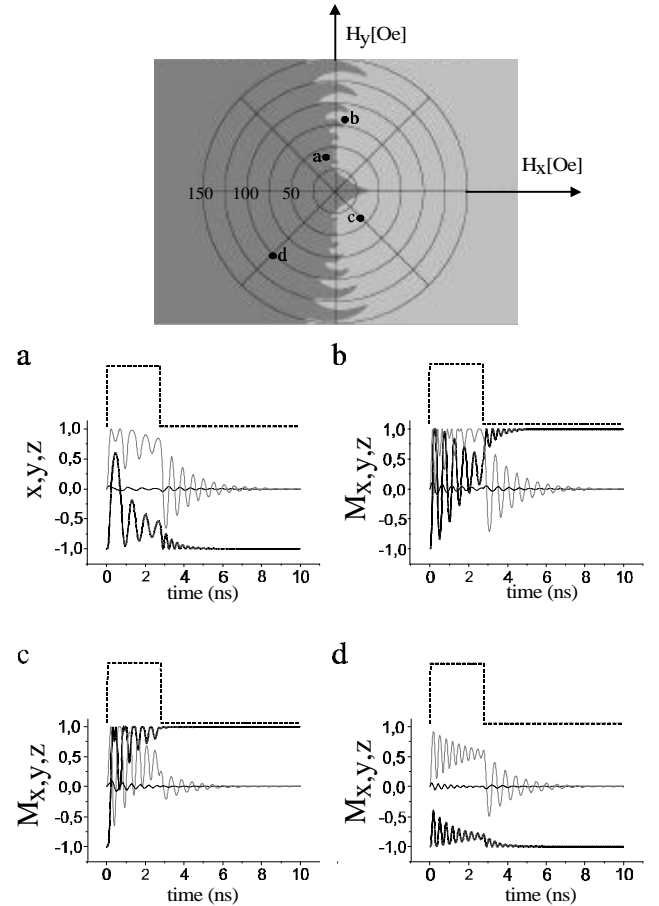

Figure 5: Switching diagram of an ellipsoidally shaped particle with the demagnetizing factors $N_x = 0.008$, $N_y = 0.012$ and $N_z = 0.980$, i.e., the x-axis is the easy magnetization axis. The initial direction of magnetization is along the $-x$-direction. A field pulse of 0/2.75/0 ns is applied. Bright (dark) areas indicate that the magnetization has switched (not switched) from the $-x$-direction into the $+x$-direction. The direction of each point of the diagram from the center indicates the direction of the applied field pulse. The strength of the field pulse is proportional to the distance from the center. The circles show increments of the field strength of 25 Oe. The four panels display the time evolution of the three magnetization components M_x (bold black line), M_y (thin gray line) and M_z (thin black line) at the positions indicated in the switching diagram. The time structure of the applied field pulse is shown by the dashed line.

values of current in both wires) or a rectangle (for different values of current in both wires) around the center. The intersections with the x- and y-axis contain the information about a possible switching of elements beneath each wire; the corner positions of the square/rectangle that of the cell where both wires cross each other. For stable operation, the intersections with the x- and y-axis should not switch, but the corner position should indicate successful switching.

Switching with short pulses – the precession dominated switching regime

Diagrams (a) – (c) of Fig. 5 indicate, that shorter field pulses can be used for successful switching of the magnetization. We will now first discuss the application of a very short, rectangularly shaped field pulse of 0.25 ns length. For moderate applied fields the pulse length is shorter than the precession period of the magnetization. Fig. 6 shows the results of the calculation. Compared to the results of long pulses (cf. Fig. 5) we observe a strongly alternating behavior in the right part of the diagram, where the x-component of the applied field is antiparallel to the initial direction of the magnetization. We find also that the regions in the left part of the diagram, where switching can occur, are strongly enlarged. Diagrams (a) – (d) illustrate the time evolution of the switching process for the same values and directions of the external field, as in Fig. 5. The final state of the magnetization of Fig. 6 (b) – (d) is the same as in Fig. 5 (b) – (d). In Fig. 6 (a) the magnetization is switched in contrast to Fig. 5 (a). This is because now the switching is dominated by precession. The time scale of the pulse is short enough to avoid the damping towards the $-x$-direction. From Fig. 5 (a) this can be expected for a pulse length between 0.2 and 0.6 ns, where the x-component of the magnetization is positive.
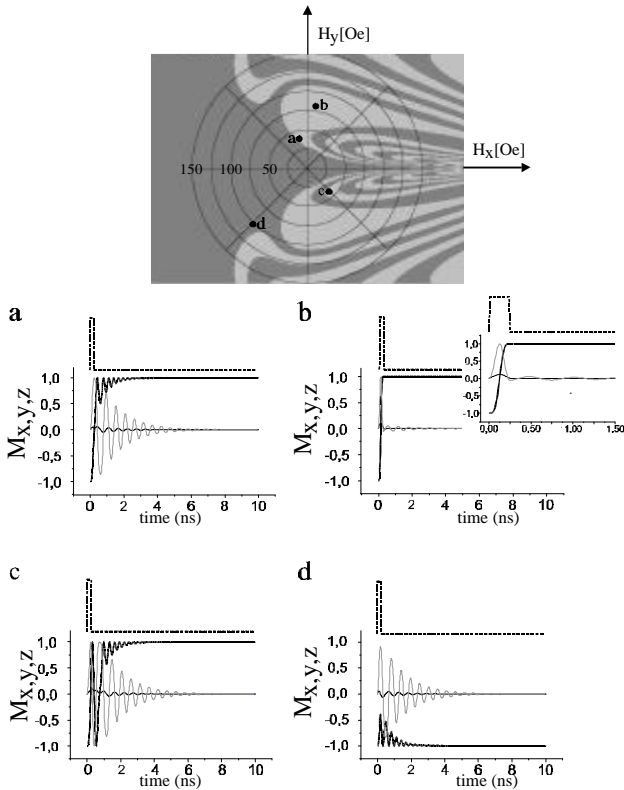
The exact values of the transition between switching and non-switching behavior cannot be extracted from Fig. 5 (a) since the path of the magnetization depends on the details of the field pulse. A remarkable situation is realized at position (b) in Fig. 6. Full switching of the magnetization is achieved within the pulse length without significant ringing afterwards. The magnetization is reversed on a time scale far beyond the relaxation time. The origin of this behavior is simply that the pulse is just switched off at the time the z-component of the magnetization crosses zero. This is energetically favorable since at this point the Zeeman energy which will be dismissed upon field termination is at maximum. In all other cases the ringing of the magnetization is qualitatively the same. For ultrafast applications the suppression of the ringing is important since only in this case consecutive pulses can be applied to the same cell without any dead time. The influence on switching stability due to different delay times between consecutive pulses can be minimized.

Figures 5 and 6 lead to the conclusion that fast switching of the magnetization can only be realized in two ways: (i) by optimization of material parameters to increase the damping parameter and (ii) switching in the precession regime as shown in Fig. 6 (b).

Influence of the shape of the magnetic field pulse on the magnetization reversal

To increase the applicability of our results to real systems we discuss next the influence of the pulse shape on the switching properties. Figure 7 summarizes the results. On the left hand side we show the diagrams for rectangularly shaped pulses in the precession limit (top, pulse length 0.25 ns, cf. Fig. 6), in the relaxation time limit (bottom, pulse length 2.75 ns, cf. Fig. 5), and in the transition regime between both limits (middle, pulse length 1.4 ns). The top and bottom diagrams on the left hand side have been discussed in detail in Fig. 6 and Fig. 5, respectively. The middle diagrams show data for a pulse length where the influences of precession and the damping term in LLG for the switching are comparable. However, in practice, pulse shapes will not be rectangular. The right panels of Fig. 7 show the switching diagrams for the same pulse lengths as in the left panels, but with rise and fall times each equal to the pulse length. In each case regions of stable switching ($+x$-direction), especially for the transition regime are enlarged compared to the case of a rectangular pulse of same duration. In addition we find that the angular range of no switching ($-x$-direction) is enlarged. Hence we find for the bottom panel on the right hand side nearly a clear separation between the switching and non-switching areas at the $\pm y$-direction except the well known Stoner asteroid in the center of the diagram for small applied fields.

To achieve stable switching for, e.g., a given range of fluctuations in material parameters, a fairly large range in the diagrams must be considered, where switching occurs. In the precession dominated case, such an area is identified along the $\pm y$-directions. Improved switching of an MRAM memory cell could be achieved by simultaneously addressing two data lines which are oriented parallel to the easy axis of magnetization, such that the generated field is oriented along the $\pm y$-directions.

Figure 6: Switching diagram for a field pulse of 0/0.25/0. All other parameters as in Fig. 5.

precession limit (pulse length = 0.25 ns)

transition regime (pulse length = 1.4 ns)

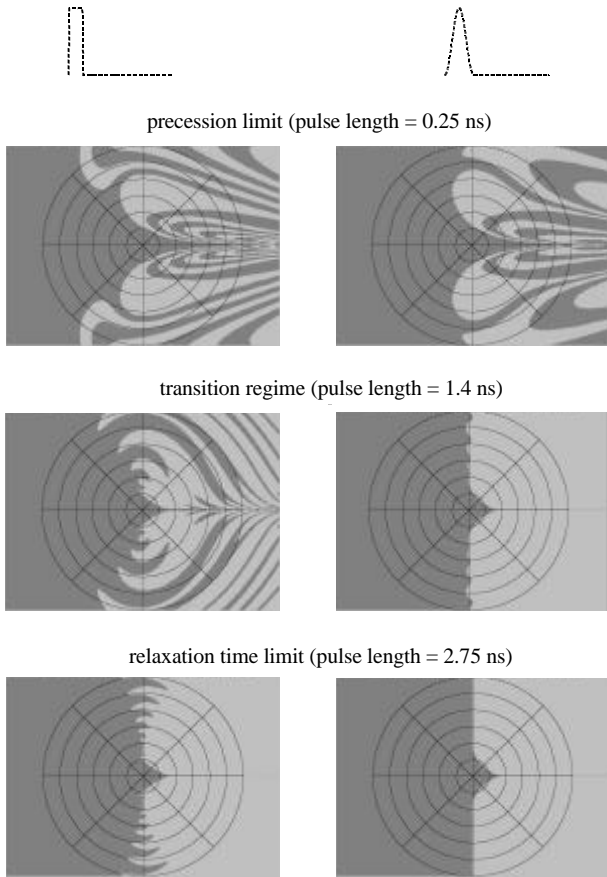
relaxation time limit (pulse length = 2.75 ns)

Figure 7: Switching diagrams as in Figs. 5 and 6 for pulse lengths of 0.25 ns (top), 1.40 ns (middle), and 2.75 ns (bottom). The left panels show the diagrams for rectangularly shaped pulses, the right panels for pulses with rise and fall times equal to the pulse length.

Summary

We have investigated the switching properties of Stoner-like magnetic particles upon application of short magnetic pulses. We find, that switching depends largely on the pulse length and the pulse shape. Two distinct switching mechanisms can be realized. For short field pulses the switching properties are governed by the precession of the magnetization whereas for long field pulses only the damping term of LLG is important. We have shown that by choosing optimum field pulse parameters the damping term is of minor importance and ultrafast switching becomes possible. Criteria for fast and stable switching are derived.

Acknowledgements

References

[1] R. Kikuchi, J. Appl. Phys. 27, 1352 (1957).

[2] L. He, W.D. Doyle, H. Fujiwara, IEEE Trans. Magn. 30, 4086 (1994).

[3] W.D. Doyle, S. Stinnet, C. Dawson, L. He, J. Magn. Soc. Jpn. 22, 91 (1998).

[4] A. Hubert, R. Schäfer, *Magnetic Domains*, Springer-Verlag, Berlin, Heidelberg (1998).

[5] M. Bauer, J. Fassbender, B. Hillebrands, to be published.

[6] M.R. Freeman, W. Hiebert, A. Stankiewicz, J. Appl. Phys. 83, 6217 (1998).

[7] C.E. Patton, Z. Frait, C.H. Wilts, J. Appl. Phys. 46, 5002 (1975).

[8] L. Landau, E. Lifschitz, Physik Z. Sowjetunion 8, 153 (1953)

[9] T.L. Gilbert, Phys. Rev. 100, 1243 (1955).

[10] J.C. Mallinson, IEEE Trans. Magn. 23, 2003 (1987).

[11] J.R. Dormand, P.J. Prince, J. Computat. and Appl. Mat. 7, 67 (1981).

[12] C.H. Back, D. Weller, J. Heidmann, D. Mauri, D. Guarisco, E.L. Garwin, H.C. Siegmann, Phys. Rev. Lett. 81, 3251 (1998).